AD

AD-E403 299

Technical Report ARMET-TR-10007

COMBINED EFFECTS ALUMINIZED EXPLOSIVES

E.L. Baker
W. Balas
C. Capellos
J. Pincay
U.S. Army ARDEC
Picatinny Arsenal, NJ 07806

L. Stiel
Polytechnic University
Six Metrotech Center
Brooklyn, NY 11201

July 2010

U.S. ARMY ARMAMENT RESEARCH, DEVELOPMENT AND ENGINEERING CENTER

Munitions Engineering Technology Center

Picatinny Arsenal, New Jersey

The views, opinions, and/or findings contained in this report are those of the author(s) and should not be construed as an official Department of the Army position, policy, or decision, unless so designated by other documentation.

The citation in this report of the names of commercial firms or commercially available products or services does not constitute official endorsement by or approval of the U.S. Government.

Destroy this report when no longer needed by any method that will prevent disclosure of its contents or reconstruction of the document. Do not return to the originator.

REPORT DOCUMENTATION PAGE	Form Approved OMB No. 0704-01-0188

1. REPORT DATE (DD-MM-YYYY)	2. REPORT TYPE	3. DATES COVERED (*From - To*)
July 2010		

4. TITLE AND SUBTITLE	5a. CONTRACT NUMBER
COMBINED EFFECTS ALUMINIZED EXPLOSIVES	5b. GRANT NUMBER
	5c. PROGRAM ELEMENT NUMBER

6. AUTHORS	5d. PROJECT NUMBER
E.L. Baker, W. Balas, C. Capellos, J. Pincay, U.S. Army ARDEC L. Stiel, Polytechnic University	5e. TASK NUMBER
	5f. WORK UNIT NUMBER

7. PERFORMING ORGANIZATION NAME(S) AND ADDRESS(ES)	8. PERFORMING ORGANIZATION REPORT NUMBER
U.S. Army ARDEC, METC Energetics, Warheads & Manufacturing Technology Directorate (RDAR-MEE-W) Picatinny Arsenal, NJ 07806-5000 Polytechnic University Six Metrotech Center Brooklyn, NY 11201	

9. SPONSORING/MONITORING AGENCY NAME(S) AND ADDRESS(ES)	10. SPONSOR/MONITOR'S ACRONYM(S)
U.S. Army ARDEC, ESIC Knowledge & Process Management (RDAR-EIK) Picatinny Arsenal, NJ 07806-5000	11. SPONSOR/MONITOR'S REPORT NUMBER(S) Technical Report ARMET-TR-10007

12. DISTRIBUTION/AVAILABILITY STATEMENT

Approved for public release; distribution is unlimited.

13. SUPPLEMENTARY NOTES

14. ABSTRACT

This paper reports on the development of theory and performance for recently developed combined effects aluminized explosives. Traditional high energy explosives used for metal pushing incorporate high loading percentages of HMX or RDX; whereas, traditional blast explosives commonly incorporate some percentage of aluminum. Although these high blast explosives produce increased blast energies, they normally produce reduced metal pushing capability due to the relatively late time aluminum reaction. Recently developed combined effects aluminized explosives achieve both excellent metal pushing and high blast energies. The excellent metal pushing capability is due to the earlier exothermic conversion of aluminum to aluminum oxide as compared to traditional blast explosives. Traditional Chapman-Jouguet detonation theory does not explain the observed detonation states achieved by these combined effects explosives. This paper demonstrates that the eigenvalue detonation theory explains the observed behavior and that both high metal pushing capability and high blast are achieved using these new explosives.

15. SUBJECT TERMS

Combined effects aluminized explosives, Aluminized explosives, Metal pushing capability, High blast energies, Aluminum, Aluminum oxide conversion, Eigenvalue detonation theory

16. SECURITY CLASSIFICATION OF:			17. LIMITATION OF ABSTRACT	18. NUMBER OF PAGES	19a. NAME OF RESPONSIBLE PERSON
a. REPORT	b. ABSTRACT	c. THIS PAGE			Dr. Ernest L. Baker
U	U	U	SAR	17	19b. TELEPHONE NUMBER (Include area code) (973) 724-5097

ACKNOWLEDGMENTS

The participation of Dr. Leonard Stiel was supported by the U.S. Army Armament Research, Development and Engineering Center (William Poulos) under the auspices of the U.S. Army Research Office Scientific Services Program administered by Battelle (Delivery Order 0354, Contract No. DAAD19-02-D-0001).

CONTENTS

INTRODUCTION

Aluminized explosives commonly used for high blast applications do not exhibit sufficient energy for metal pushing compared to other high percentage HMX or RDX explosives (PAX-2A, LX-14, Comp A5). This is because the conversion of aluminum to aluminum oxide, which provides much of the energy output in work, occurs at much later times than the organic (H-C-N-O) reactions for the formation of the other gaseous and solid products. Recently, new aluminized explosive formulations using small aluminum particles were developed to produce high initial detonation temperatures, pressures, and velocities. These new aluminized explosives exhibit high work output energies at much earlier volume expansions. Therefore these new "combined effects" explosives exhibit both excellent early volume expansion metal pushing and high expansion blast capabilities. These explosives include PAX-29 (77 weight % CI-20 and 15 % Al), PAX-30 (77 weight % HMX and 15 % Al), and PAX-42 (77 weight % RDX and 15 % Al) (ref. 1). In order to understand and simulate the behavior of these explosives, a model was developed in this study that accounts for the essential features exhibited, including fast but delayed aluminum oxidation reactions upon detonation. Relationships are also described that enable the implementation of the model for the prediction of detonation properties.

BACKGROUND

JAGUAR analytical procedures were developed for the accurate calculation of detonation properties of high-blast aluminized explosives. These routines are an extension of the EXP-6 thermochemical equation of state procedures developed for JAGUAR for H-C-N-O explosives. Relationships for the melting curves of aluminum and aluminum oxide are used to identify the correct phases present at every calculation point. For a number of aluminized explosives, detonation velocities calculated with JAGUAR and the assumption of little or no aluminum reaction are consistent with recent experimental values to within the accuracy of the data and the analytical procedures used (refs. 2 and 3). For most of the explosives studied, the calculated detonation velocities decrease slightly in the range 0 to 25% aluminum reaction, and are substantially lower for 100% reaction.

The analyses of cylinder test data indicate that with the use of large particles of 50 μm and higher, such as for the U.S. Army Armament Research, Development and Engineering Center (ARDEC), Picatinny Arsenal, New Jersey measurements for PAX-3 (an HMX based explosive with 20 weight % aluminum), little or no reaction occurs for more than 10 volume expansions. For an analytic cylinder model, best agreement with cylinder expansion tests for several explosives with small aluminum particles is obtained by the assumption of complete aluminum reaction throughout the principal isentrope (refs. 5 to 7). For BTNEN with 15 weight % aluminum, Gogulya et al (refs. 4 and 8) found that highest cylinder velocities are obtained with aluminum particles in the range 3 to 15 μm, with no improvement for sub-micron particles because of their increased aluminum oxide content. At the same initial density, considerably lower cylinder velocities resulted with 150 μm particles.

EIGENVALUE DETONATION MODEL

In order to account for the observed behavior of the new combined effects explosives with small aluminum particles, a model is postulated in which the explosive expands through a reaction zone at constant detonation velocity until 100% aluminum reaction is attained. At the zero aluminum reaction Hugoniot, the aluminum is un-reacted while the other gaseous and solid C-H-N-O products are in equilibrium. For the partially reacted aluminum Hugoniots, the reacted aluminum fraction detonation product (aluminum oxide) is in equilibrium with the other C-H-N-O products. The reasoning behind this construct is that the organic reactions are significantly faster than the time required for the aluminum to react. For the reaction zone, a standard assumption is adopted, where the necessary Hugoniot and Rayleigh line relationships are satisfied. However, it has been noted that for the aluminized explosives investigated to date, the un-reacted aluminum Hugoniot actually lies above the reacted aluminum Hugoniots. For this reason, the minimum detonation velocity solution (and minimum entropy solution) occurs with the Raleigh line intersecting the zero aluminum reaction Hugoniot at the tangency point. Figure 1 presents a graphical depiction of the associated Hugoniots and Rayleigh line. The associated detonation velocity is the velocity that would be measured in experimentation. This type of detonation is known in the literature as an eigenvalue detonation (ref. 9). The eigenvalue detonation velocity, which is consistent with the measured detonation velocity, is determined by the tangency of the Rayleigh line to the un-reacted Hugoniot curve.

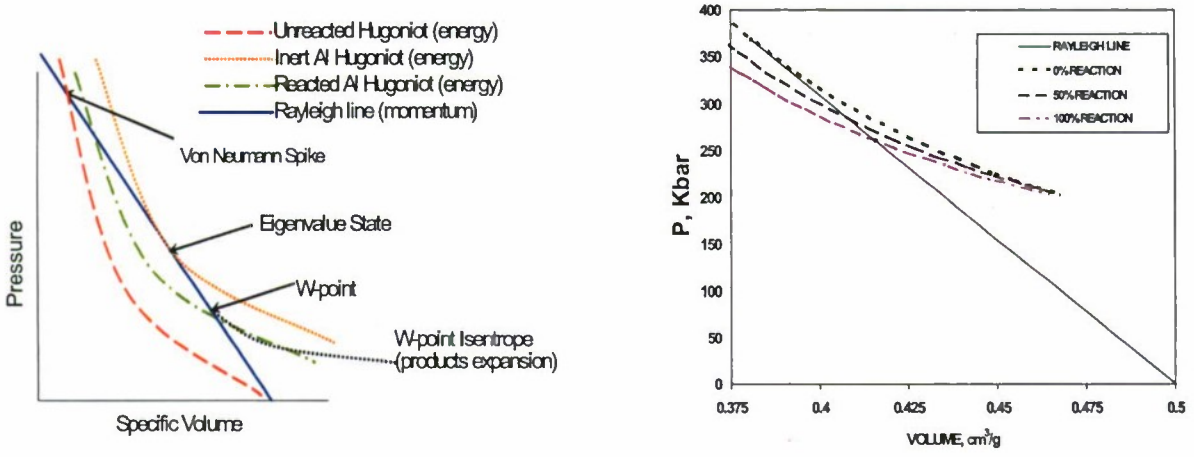

Figure 1
Eigenvalue detonation (left) and Hugoniot curves for PAX-29 (right)

In figure 1, Hugoniot curves are presented for PAX-29 at an initial density of 1.999 g/cm^3 for 0, 50, and 100% of reacted aluminum. At this density with micron-size particles, the detonation velocity measured by cylinder tests at ARDEC is 8.95 km/s. For zero aluminum reaction, the initial detonation point is at P = 368 kbar and T = 3519 K. The calculated eigenvalue detonation velocity for zero aluminum reaction (8.78 km/s) is attained on the Hugoniot curve for 100% reaction at P = 260 kbar and T = 4699 K. This point is designated as the "W-point," since it corresponds to a weak intersection of the Rayleigh line with the Hugoniot curve. The W-point conditions compare with those of the never achieved 100% aluminum reaction Chapman-Jouguet (C-J) point for which the calculated detonation velocity is 8.21 km/s: P = 358 kbar and T = 4955 K. Since the calculated entropies are very similar at the W-point and at the 100% reaction C-J point, almost identical energies on the isentropic expansion curve result from either starting point (refs. 2 and 5).

Hugoniot curves for PAX-30 (initial density 1.909 g/cm^3) are shown in figure 2. The point of tangency of the Rayleigh line with the zero aluminum reaction Hugoniot is at P = 352 kbar and T = 3119 K. The calculated detonation velocity at this initial point is 8.43 km/s, compared to the experimental detonation velocity from ARDEC cylinder tests, 8.51 km/s. The W-point conditions on the 100% aluminum reaction Hugoniot are P = 246 kbar and T = 4235 K. For reference, the never achieved 100% reaction C-J point has a calculated detonation velocity of 8.06 km/s.

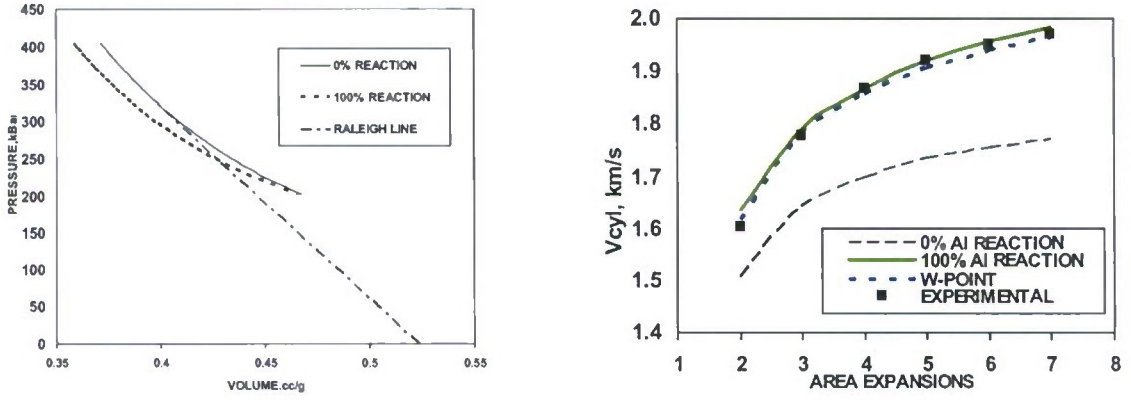

Figure 2
Hugoniot curves PAX-30 (left) and cylinder velocities of PAX-29 (right)

New JAGUAR procedures were developed to enable the determination of the W-point conditions for an aluminized explosive. At a specified initial density, the W-point is established as the point on the 100% reaction Hugoniot curve, which exhibits the same detonation velocity as that established for zero reaction. The detonation velocity at each Hugoniot point is calculated as

$$D = \sqrt{\frac{V_R(P-P_R)}{1-V^*}} \tag{1}$$

where P_R and V_R are the pressure and specific volume at the reference state, and V^* is the relative volume V/V_R.

CYLINDER VELOCITY MODEL

The variation of the P-V* curve for isentropic expansion from the W-point is empirically represented by a relationship of the Jones-Wilkins-Lee-Baker (JWLB) form

$$P = \sum_i A_i e^{(-R_i V^*)} + CV^{*-(\omega+1)} \tag{2}$$

The constants of these JWLB relationships are established by the non-linear quadratic programming-Ernest Baker (NLQPEB) variable metric optimization routines (ref. 10). For the parameterization of the isentropic P-V* relationship, equation 2, A_i, R_i R_i, and C variables are constrained to be positive, and the W-point pressure resulting from the JWLB relationship is constrained to be equal to the JAGUAR value. The JWLB constants for aluminized explosives are used to calculate cylinder expansion velocities with an analytic cylinder test model (ref. 11). Isentropic expansion is assumed for the detonation products from the W-point state. In addition, constant detonation products are assumed across spherical surfaces, which perpendicularly intersect the cylinder inside wall. The products mass velocities are assumed perpendicular to the spherical surfaces. These assumptions - along with mass, momentum, and energy conservation - result in the final model.

In figure 2, the cylinder velocities calculated using the JWLB constants for the W-point approach are compared with the corresponding experimental values for PAX-29. The ARDEC data for PAX-29 with micron size particles were obtained with 1-in. cylinders (ref. 12), and represent the average values for experimental runs with an average initial density of 2.0 g/cm^3. The experimental cylinder velocities are high and indicate substantial reaction for most of the expansion range. The values calculated with the analytical relationships for expansion from the W-point are in reasonable agreement with the experimental values. The cylinder velocities with the W-point relationships are slightly lower than the corresponding values resulting with the analytic cylinder model and the JWLB relationships for the principal isentrope from the 100% reaction C-J point. At seven area expansions, the average experimental velocity is 1.97 km/s, the value for expansion from the 100% reaction C-J point is 1.985 km/s, and the velocity for the W-point expansion is 1.965 km/s. Similar comparisons were performed for PAX-30 with 15 weight % aluminum. The experimental values are an average of experimental tests at an initial density of 1.885 g/cm^3 with micron size aluminum particles. The experimental cylinder velocities are high for most of the expansion range. In figure 3, it can be seen that the calculated cylinder velocities for expansion from the W-point are in good agreement with the experimental values for most of the expansion range. The calculated values for the 100% aluminum reaction principal isentrope are slightly higher than the W-point calculated values at high expansions. In figure 3, comparisons are presented for PAX-42 for an initial density of 1.827 g/cm^3. The calculated velocities for expansion from the 100% Al reaction C-J point or from the W-point are seen to agree with the experimental values mentioned, about three area expansions.

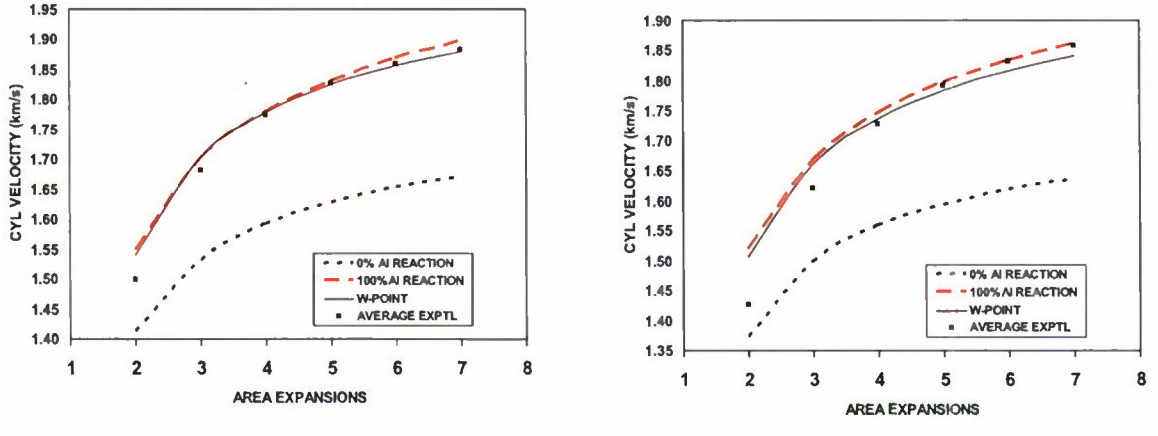

Figure 3
Cylinder velocities for PAX-30 (left) and PAX-42 (right)

Cylinder velocities for PAX-29, PAX-30, and PAX-42 calculated with JAGUAR and the analytical cylinder W-point model are consistent with the experimental values for radial cylinder expansions greater than about 4 to 5 mm of cylinder wall movement, corresponding to elapsed times of 3 to 4 μs. The actual times for the completion of the aluminum reaction are very likely to be considerably smaller, due to model and experimental uncertainties at these very early times. As seen in figure 4, cylinder velocities for PAX-3 with large aluminum particles are consistent with the calculated values for zero aluminum reaction for a wide range, including very early volume expansions (ref. 2).

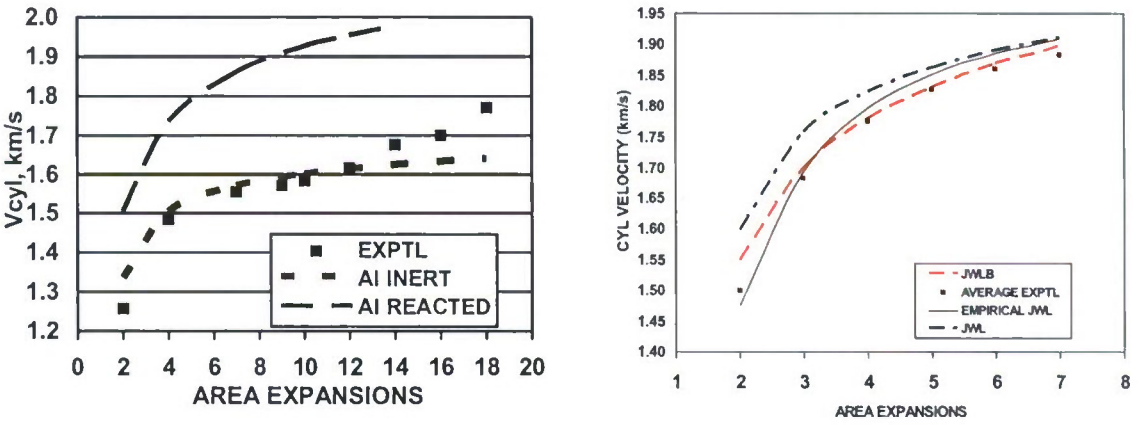

Figure 4
Cylinder velocities for PAX-3 (left) and an empirical PAX-30 JWL (right)

THERMODYNAMIC EQUATIONS OF STATE

The JWLB and Jones-Wilkins-Lee (JWL) equations of state were parameterized for combined effects explosives using fairly conventional methodology. The P-V* behavior for the principal isentrope is represented by the JWLB relationship as

$$P = \sum_{i=1}^{5} A_i e^{(-R_i V^*)} + C V^{*-(\omega+1)} \tag{3}$$

As before, the constants of the JWLB equation of state are established by NLQPEB variable metric optimization routines. The constant ω in equation 3 is determined from the variation of the Gruneisen parameter λ with V^* through the relationship

$$\lambda = \sum_{i} (A_{\lambda i} V^* + B_{\lambda i}) e^{-R_{\lambda i} V^*} + \omega \tag{4}$$

The equation of state detonation velocity and pressure are calculated from the W-point procedure as presented previously. The associated JWLB equation of state parameters is presented in table 1. It is important to realize the presented equations of state are intentionally inconsistent. That is to say that the presented detonation velocities and pressures purposely do not agree with the calculated C-J state associated with the equation of state constants but agree rather with the W-point. In this way, the under-driven W-point is achieved in hydrocode applications. It is also important to realize that if a different burn routine is attempted (volume or beta burn), the under-driven W-point will not be achieved. In hydrocodes that check for equation of state consistency (CALE, CTH), a warning message will appear informing the user that the inserted detonation velocity (W-point) does not agree with the calculated C-J state. Such warning messages should be ignored when using these JWLB and JWL equations of state representing eigenvalue detonation behavior.

Table 1
JWLB parameters for combined effects explosives

	PAX-3 (Al INERT)	PAX-29	PAX-30	PAX-42
$\rho 0$ (g/cm^3)	1.866	1.999	1.885	1.8265
E0 (Mbar)	0.082047	0.14716	0.13568	0.13109
D (cm/μs)	0.8049	0.8784	0.8342	0.8137
P (Mbar)	0.2939	0.2599	0.2419	0.2339
A1 (Mbar)	399.991	400.407	406.224	400.717
A2 (Mbar)	10.3055	82.630	135.309	16.5445
A3 (Mbar)	2.8756	1.5507	1.5312	1.45169
A4 (Mbar)	0.0321197	0.006126	0.006772	0.006103
R1	13.5562	20.9887	26.9788	13.6945
R2	7.70458	9.6288	10.6592	8.67402
R3	3.37987	2.42441	2.52342	2.5320
R4	0.920167	0.328128	0.335585	0.33570
C (Mbar)	0.007651	0.014626	0.013561	0.014057
ω	0.280167	0.24286	0.234742	0.242371
Aλ1	60.7701	60.6372	72.6781	73.0820
Aλ2	11.2185	6.12950	5.64752	5.45602
Bλ1	6.99635	3.24383	2.87280	2.72707
Bλ2	-7.26845	-3.48268	-3.10754	-2.85672
Rλ1	26.7932	24.2892	27.8109	27.4611
Rλ2	1.99336	1.68684	1.71375	1.74770

The cylinder velocities calculated with the analytic cylinder procedures and JWLB equation of state parameters are about 3% lower at two area expansions than for the corresponding calculations with JWL parameters. The results of studies with CALE hydrocode procedures (ref. 6) indicate that the JWLB procedure is required to obtain accurate information about the onset of aluminum reaction from cylinder test information. In figure 4 for PAX-30, larger deviations from the experimental cylinder velocities are seen at low expansions for the JAGUAR JWL relationship with 100% aluminum reaction. Empirical JWL parameters were obtained by analytic cylinder procedures that reproduce the experimental cylinder velocities for the entire expansion range, as shown in figure 4 for PAX-30. The empirical JWL parameters for PAX-29, PAX-30, and PAX-42 are presented in table 2, along with the actual JWL parameters for LX-14 and PAX-2A.

Table 2
JWL parameters for high energy and combined effects explosives

	LX14	PAX-2A	PAX-29	PAX-30	PAX-42
ρ0 (g/cc)	1.819	1.770	1.999	1.885	1.827
E0 (Mbar)	0.10213	0.09953	0.14714	0.135755	0.12994
D (cm/μs)	0.8630	0.8391	0.8784	0.8342	0.8137
P (Mbar)	0.3349	0.3124	0.2599	0.2419	0.2339
A1 (Mbar)	26.1406	27.0134	8.58373	7.19151	13.8484
A2 (Mbar)	0.763619	.762675	0.168261	0.097112	0.145102
R1	6.93245	7.22237	4.7726	4.59098	5.74864
R2	1.94159	1.95979	1.03613	0.84089	0.99404
C (Mbar)	0.010994	0.010919	0.014556	0.013492	0.015193
ω	0.384193	0.375812	0.242252	0.233665	0.253095

CONCLUSIONS

The new combined effects aluminized explosives PAX-29, PAX-30, and PAX-42 exhibit high detonation velocities and pressures, as well as high work energies for both low and high volume expansions. The model postulated in this study represents the observed behavior for the detonation properties of these explosives. The presented JWLB and JWL equations of state can be used in hydrocode applications to reliably produce eigenvalue W-point detonation and expansion behavior. It is important to realize the eigenvalue W-point is an under-driven state on the fully reacted aluminum Hugoniot for a given explosive and does not represent traditional Chapman-Jouguet sonic conditions. It appears that with small aluminum particles, appreciable aluminum reaction does not occur at the reaction zone front, which establishes the detonation velocity for the reaction zone. This zero aluminum reaction detonation velocity is observed in the time frame of experimental measurements. The organic detonation products are considered to reach chemical equilibrium at the reaction zone front. Complete aluminum reaction is then attained in a short time after the initial point. This is in contrast to an explosive incorporating large aluminum particles (such as PAX-3), where the gaseous products expand to low pressures before significant aluminum reaction takes place. Other important contributing factors to early reaction aluminum participation appear to be characteristic melt times for the aluminum particles and available oxidizer percentage (refs. 6 and 7).

REFERENCES

1. Balas, W.; Nicolich, S. Nicolich; Capellos, C.; Hatch, R.; and Braithwaite, P., "New Aluminized Explosives for High Energy, High Blast Warhead Applications," Proceedings 2006 Insensitive Munitions & Energetic Materials Technology Symposium, Bristol, UK, 24-28, April 2006.

2. Stiel, L.I.; Baker, E.L.; and Capellos, C.; "JAGUAR Analyses of Experimental Detonation Values for Aluminized Explosives in Shock Compression of Condensed Matter," (M.D. Furnish, Y.M. Gupta, and J.W. Forbes eds.), part II, pp. 891-894, 2003.

3. Baker, E.L.; Capellos, C.; and Stiel, L.I., "Stable Detonation Velocities for Aluminized Explosives," Sci. Tech. Energ. Mat. 67, No. 4, pp. 134-138, 2006.

4. Gogulya, M.F.; Dolgoborodov, A.Yu; Brazhnikov, M.A.; and Baudin, G., "Detonation Waves in HMX/Al Mixtures (Pressure and Temperature Measurements)," Proceedings of the Eleventh International Detonation Symposium, ONR 33300-5, Arlington ,VA, pp. 979-988, 1998.

5. Stiel, L.I.; Capellos, C. Capellos; and Baker, E.L. Baker; "Study of Detonation Velocities and Cylinder Velocities for Aluminized Explosives in Shock Compression of Condensed Matter," (M.D. Furnish , M. Elert, T.P. Russell, and C. T. White, eds.), part I, pp. 475-478, 2005.

6. Baker, E.L.; Capellos, C.; and Stiel, L.I.; "Generalized Thermodynamic Equation of State for Reacting Aluminized Explosives," 13th Int. Detonation Symp., Norfolk,,VA, July 23-28, 2006.

7. Capellos, C.; Baker, E.L.; Nicolich, S.; Balas, W.; Pincay, J.; and Stiel, L.I. Stiel, "Eigenvalue Detonation of Combined Effects Aluminized Explosives," Proceeding of the 15th APS Topical Conference on Shock Compression of Condensed Matter, Kohala Coast, Hawaii, 24-29 June 2007.

8. Gogulya, M.F.; Dolgoborodov, A.Yu; Makhov, M.N.; Brazhnikov, M.A.; and Shetinin, V.G. Shetinin, "Detonation Performance of Aluminized Compositions Based on BTNEN," Proceeding of the 12th Int. Detonation Symp., San Diego, CA, August 2002.

9. Fickett, W. and Davis, W.C., Detonation, University of California Press, Berkeley, California, 1979.

10. Baker, E.L., "An Application of Variable Metric Nonlinear Optimization to the Parameterization of an Extended Thermodynamic Equation of State," Proc. Tenth International Detonation Symposium, ONR 33395-12, Arlington, VA, pp. 394-400, 1993.

11. Baker, E.L., "Modeling and Optimization of Shaped Charge Liner Collapse and Jet Formation," Technical Report ARAED-TR-92019, U.S. Army Armament Research, Development and Engineering Center, Picatinny Arsenal, NJ, January, 1993.

12. Fuchs, B.E., "Picatinny Arsenal Cylinder Expansion Test and a Mathematical Examination of the Expanding Cylinder," Technical Report ARAED-TR-95014, U.S. Army Armament Research, Development and Engineering Center, Picatinny Arsenal, NJ, October 1995.

DISTRIBUTION LIST

U.S. Army ARDEC
ATTN: RDAR-EIK
RDAR-GC
RDAE-MEE-W, E. Baker
Picatinny Arsenal, NJ 07806-5000

Defense Technical Information Center (DTIC)
ATTN: Accessions Division
8725 John J. Kingman Road, Ste 0944
Fort Belvoir, VA 22060-6218

Commander
Soldier and Biological/Chemical Command
ATTN: AMSSB-CII, Library
Aberdeen Proving Ground, MD 21010-5423

Director
U.S. Army Research Laboratory
ATTN: AMSRL-CI-LP, Technical Library
Bldg. 4600
Aberdeen Proving Ground, MD 21005-5066

Chief
Benet Weapons Laboratory, WSEC
U.S. Army Research, Development and Engineering Command
Armament Research, Development and Engineering Center
ATTN: RDAR-WSB
Watervliet, NY 12189-5000

Director
U.S. Army TRADOC Analysis Center-WSMR
ATTN: ATRC-WSS-R
White Sands Missile Range, NM 88002

Chemical Propulsion Information Agency
ATTN: Accessions
10630 Little Patuxent Parkway, Suite 202
Columbia, MD 21044-3204

GIDEP Operations Center
P.O. Box 8000
Corona, CA 91718-8000